VOL. 18, NO. 10 AIAA JOURNAL OCTOBER 1980

ARTICLE NO. 79-1557R

Shock-Free Wing Design

K-Y. Fung,* H. Sobieczky,† and R. Seebass‡
University of Arizona, Tucson, Ariz.

A simple numerical method for generating wing shapes that will be shock free at a specified supercritical Mach number is described. The method involves using a fictitious gas law for the supersonic domain to make the governing equations elliptic. Requirements on this gas law are detailed and a method for computing the real flow in the supersonic domain, given initial data on the embedded sonic surface, is described. The failure of the method to yield a shock-free flow when a limit surface occurs in the supersonic flow, and the difficulties that arise because the initial-value problem for the supersonic domain is ill-posed, are delineated. Finally, a small perturbation algorithm is used to illustrate the procedure and results are given for a simple baseline wing.

Introduction

INCREASED fuel efficiency, and in the case of commercial aircraft, productivity, can be achieved by operating aircraft at supercritical Mach numbers, provided that shock waves can be avoided or made acceptably weak. Two-dimensional procedures for prescribing airfoil sections that are shock free have already provided improvements in aircraft efficiency by employing these airfoils on swept wings. Three-dimensional effects have compromised such designs to some extent, and extensive wind tunnel development tests have been required to recapture the benefits of these "supercritical airfoils."

Sobieczky et al.[1] demonstrated a method of modifying baseline configurations so that they would be shock free at a prescribed Mach number and lift coefficient. This procedure provides a special opportunity for improving aircraft performance through a careful selection of the baseline configuration in order to provide wings and wing-body combinations that are shock free at supercritical Mach numbers, and that have acceptable off-design performance. Yu[2] and Yu and Rubbert[3] have also documented that this procedure is possible and demonstrated its application.

As was first described by Sobieczky,[4] a numerical algorithm is used to solve a fictitious set of equations for the flow past the baseline configuration. These equations are identical to the correct equations for subsonic portions of the flow, but they are modified when the flow becomes supersonic, so that even though the flow speed is larger than the local speed of sound the equations themselves remain elliptic. This procedure generates a numerical solution that satisfies the appropriate equations where the flow is subsonic, and the appropriate boundary conditions on the configuration outside of the supersonic zone. The results of this calculation provide the flowfield at the sonic surface. This surface and flowfield define an ill-posed initial value problem for the supersonic domain that is to be solved using the correct equations. Because this problem is ill-posed in three dimensions any numerical method must, in principle, be unstable. This instability, however, is of no consequence for moderate to high aspect ratios. However, if the detailed definition of the spanwise modifications required to make the wing shock free are comparable to those for the streamwise direction, as they will be for low aspect ratios, then the instability may compromise the calculations.

Presented as Paper 79-1557 at the AIAA 12th Fluid and Plasma Dynamics Conference, Williamsburg, Va., July 23-25, 1979; submitted Aug. 13, 1979; revision received March 25, 1980.

Index categories: Aerodynamics; Transonic Flow; Configuration Design.

*Research Assistant Professor. Member AIAA.

†Adjunct Professor, also Research Scientist, DFVLR, Göttingen, West Germany. Member AIAA.

‡Professor. Associate Fellow AIAA.

Fictitious Equations

The flows we seek are to be shock free. As a consequence, they will be irrotational and the governing equation will be the conservation of mass, viz.,

$$\nabla \cdot (\rho \nabla \phi) = 0 \tag{1}$$

where

$$\rho/\rho_* = \left\{1 + \frac{\gamma-1}{2}\left[1 - (\nabla\phi)^2/a_*^2\right]\right\}^{1/(\gamma-1)} \tag{2}$$

or

$$\nabla\phi \cdot \nabla \frac{(\nabla\phi)^2}{2} - a^2 \nabla^2 \phi = 0 \tag{3}$$

where

$$a^2 = a_*^2 + \frac{\gamma-1}{2}\left[a_*^2 - (\nabla\phi)^2\right] \tag{4}$$

Here $(\,)_*$ refers to the critical flow conditions where $q=a$. While the conservative formulation, Eq. (1), is to be preferred over its nonconservative analog, Eq. (3), numerical computations using Eq. (3) should be satisfactory provided that the flow being computed has no shock waves.

In order to generate smooth data on embedded sonic surfaces that are potentially consistent with shock-free flow, we elect to modify the gas laws (2) and (4) so that Eqs. (1) and (3) remain elliptic when $q \geq a_*$. Thus we require

$$\frac{\partial(\rho_f q)}{\rho_f \partial q} > 0 \quad \text{if } q > a_* \tag{5a}$$

or

$$a_f > q \quad \text{if } q > a_* \tag{5b}$$

where ρ_f and a_f are a fictitious density and a fictitious sound speed and the partial derivative in Eq. (5a) is taken along a streamline. If we restrict ρ_f and a_f to be functions of q alone, then

$$\frac{\rho_f}{\rho_*} = \exp\left[-\int_{a_*}^{q} \frac{q\,dq}{a_f^2(q)}\right]$$

The choice of the fictitious equation or gas law is a tool or technique available to produce a range of designs that are shock free; the initial data found with one gas law may lead to

a limit surface above the wing, while that with another gas law will not. The main consideration in choosing the fictitious equations is that the equation must imply a conservation law and that the conserved quantity must be identical to the mass flux at sonic flow conditions. This insures that the initial data for the supersonic domain is consistent with the conservation of mass in the subsonic flow.

Examples of fictitious gas laws which lead to an elliptic equation include:

$$\rho_f/\rho_* = (a_*/q)^P, \text{ or } a_f = P^{-1/2} q, \quad P<1$$

$$\rho_f/\rho_* = \exp\{1/L[(a_*/q)^L - 1]/L\}, \text{ or } a_f = q(q/a_*)^{L/2}, L>0$$

$$\frac{\rho_f}{\rho_*} = \left[\frac{a_*^2}{q^2+\mu(q^2-a_*^2)}\right]^{\frac{1}{2(1+\mu)}}, \text{ or } a_f^2 = q^2+\mu(q^2-a_*^2), \quad \mu>0$$

These gas laws are all of the simple form $\rho=\rho(q)$. It may sometimes be of value to consider an equation that has an explicit spatial dependence in order to alter the shape of the sonic domain. If this is done, care must be taken to insure that a conservation law is implied. Thus we may use $\rho_f=\rho_f(x,y,z)$ and be sure a mass flux is conserved but not, in general, $a_f=a_f(x,y,z)$.

Supersonic Domain

Given a suitable numerical algorithm for solving Eqs. (1) or (3), with the fictitious density or sound speed used for supercritical speeds, we may then locate the embedded surface where $q=a$, and evaluate the velocity components there. Those may be the physical components, viz., u, v, w in the Cartesian coordinates x, y, z or the components U, V, W, in some mapped space X, Y, Z. Because the equations are hyperbolic we choose to work with a first-order system

$$(a^2-u^2)u_x + (a^2-v^2)v_y + (a^2-w^2)w_z - 2uww_x - 2uvv_x - 2vwv_z = 0 \tag{6}$$

$$w_x - u_z = 0, \quad w_y - v_z = 0, \quad (u_y - v_x = 0) \tag{7}$$

with one of the three irrotationality conditions being redundant.

We must then set up a suitable numerical algorithm for the computation of the supersonic flow, marching inward in some fashion toward higher Mach numbers until the stream surface upon which the supersonic surface rests can be continued. In the process two difficulties may arise. The first is that the computation may indicate that the solution has become multivalued because a limit surface intervenes between the sonic surface and the body; then no physically acceptable solution is possible with the initial data supplied. The second is that the inherent instability of the algorithm may become manifest, providing an unacceptable solution. We discuss this problem further shortly.

A nonsubstantive difficulty that may arise with an approach using rectangular coordinates is due to the topology of the supersonic domain. We can expect the supesonic region to wrap around, or more picturesquely, "grab," the wing leading edge, as shown in Fig. 1a. When this occurs, one of the derivatives in the two equations selected from Eqs. (7) may vanish, leading to a singular system of equations. This is most easily avoided by mapping the solution domain to a coordinate system in which this does not occur, as discussed in Ref. 5. The coordinate systems of the computational algorithms to be used may provide the essentials of the mapping. Thus the coordinate systems used in the computational algorithms of Jameson and Caughey[6] and Caughey and Jameson[7] provide natural coordinate systems

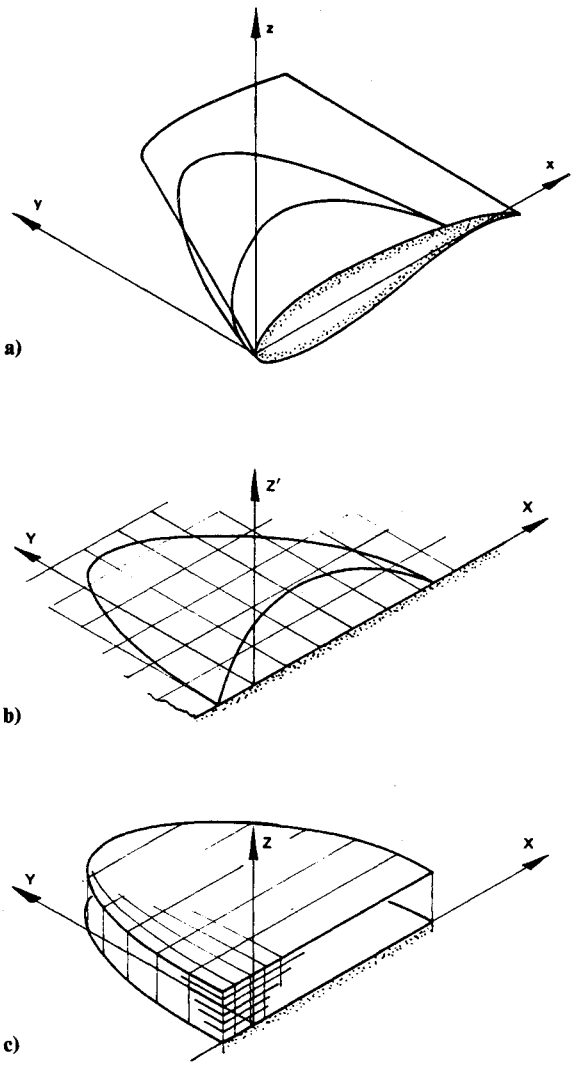

Fig. 1 Local supersonic region in the physical and computational domains.

for the computation of the supersonic domain. In the first of these the wing surface is mapped to the plane $Z'=0$, and we may envision the sonic surface to be as depicted in Fig. 1b.

A subsequent mapping

$$Z = Z'/Z'_*(X,Y)$$

where $Z'_*(X,Y)$ is the sonic surface, then leads to a computational domain like that sketched in Fig. 1c.

In this domain, with U, V and W the X, Y and Z components of the velocity derived from some appropriate potential, we have a system of equations of the form

$$AU_X + BU_Y + CU_Z = 0$$

which we use to advance the solution from one Z level k to the next:

$$U_k = U_{k-1} + [(C^{-1}A)_{k-1/2}(U_X)_{k-1/2} + (C^{-1}B)_{k-1/2}(U_Y)_{k-1/2}]\Delta Z$$

Here we use the subscript $k-1/2$ to indicate a suitably iterated average value of the subscripted quantity and ΔZ is the decrement in the Z coordinate. At each Z station the X and Y derivatives of U are calculated using three-dimensional cubic splines to specify U. Presumably the spline used should be one that avoids introducing, or perhaps even filters out, oscillations in the numerical results.

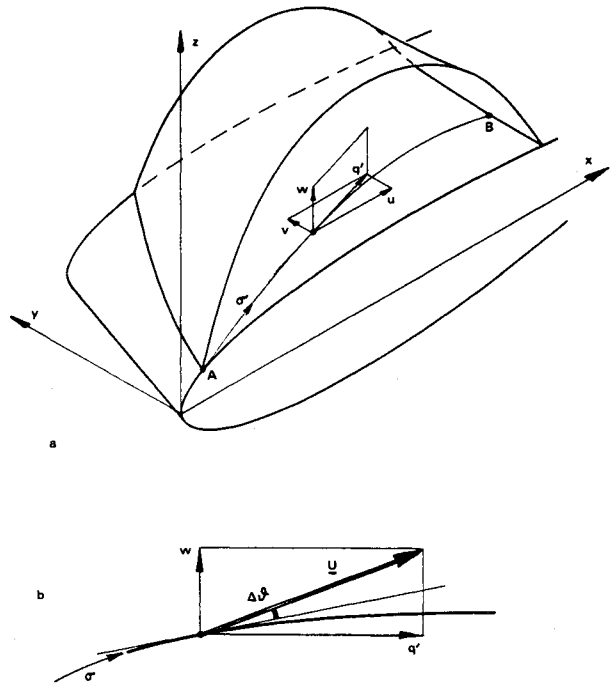

Fig. 2 Change in the flow inclination on the original wing surface that is used to define the new wing surface.

The calculation of U proceeds from one Z level to the next until the original wing surface, in this example $Z=0$, is reached. A new stream surface is then extrapolated from the values of U there, or the computation may be pushed further, to negative Z, and the new stream surface interpolated from the additional values so calculated. If we simply wish to extrapolate the new body surface we may do so in the original physical coordinates x, y, z, or in the mapped coordinates X, Y, Z.

In the original coordinates we may use the new velocity field on the original body (u_b, v_b, w_b) to define the slope in the stream direction,

$$\tan\theta_b = w_b/\sqrt{u_b^2+v_b^2} = w_b/q'$$

As sketched in Fig. 2, the local stream direction is then determined in order to integrate the angular difference $\Delta\theta(\sigma)$ along the arc length σ from A to B. The new body surface may be constructed by marching in the downstream (or upstream) direction and using a cubic spline in the spanwise coordinate to define the body at the computational nodes.

This procedure assumes small surface deviations so that the velocity field's initial surface is also that of the new surface. Extrapolation of the results on the initial surface, and an iterative correction of the new surface found, may be carried out if higher accuracy is required.

Limit Surfaces

Shock-free designs are not always possible for a given baseline configuration, Mach number, and lift coefficient. The initial data generated by given fictitious equations may imply a multivalued solution before the body stream surface intervenes. When this occurs a limit surface will be found in the flowfield. The first occurrence of a limit surface is along a line where U_Z, V_Z, $W_Z=\infty$; the algorithm used to compute the supersonic domain should be constructed so that it can recognize when this occurs, otherwise results may be obtained that have no meaning. Such a surface might look like that sketched in Fig. 3.

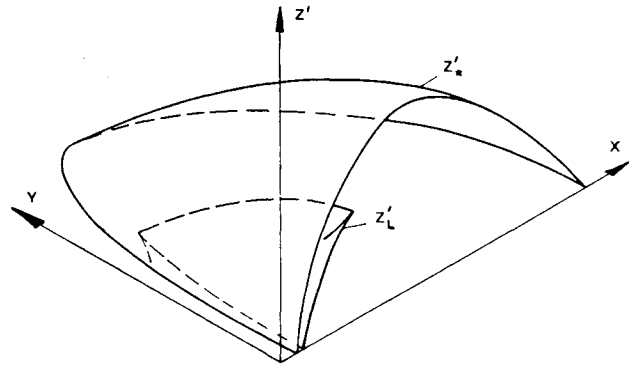

Fig. 3 Sonic surface with a limit surface embedded in the supersonic region.

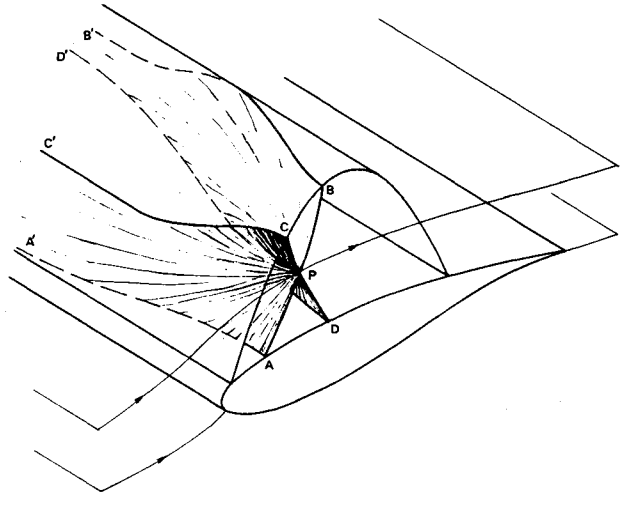

Fig. 4 Sketch of Mach conoids for a two-dimensional flow.

Initial Value Problem

As we mentioned earlier, the initial value problem for the supersonic domain is ill-posed in three dimensions. That is, small changes in the initial data will cause large changes in the solution in the domain of the problem. If we return to the well-posed two-dimensional problem and consider it to be a three-dimensional problem with no variations in the third direction, then we may sketch the Mach conoids, as shown in Fig. 4. The fore and aft Mach conoids define the influence and dependence domains of P. Because we find shock-free solutions the flow is reversible and we may consider the time-like direction to be in either the $\pm q$ direction. When we calculate the solution at P using data from the sonic surface we are effectively replacing the data along AA' by that along BB'. Alternatively, in two dimensions, the normal to the streamline may also be considered time-like and we calculate the solution at P using the data on CB. In three dimensions this alternative approach fails because the solution at P now depends upon the infinite domain $CC'B'B$.

An informative simple example is that of the linear wave equation

$$-\phi_{xx}+\phi_{yy}+\phi_{zz}=0$$

with data given on the $z=0$ plane as sketched in Fig. 5; viz.,

$$\phi(x,y,0)=f(x,y), \qquad \phi_z(x,y,0)=g(x,y)$$

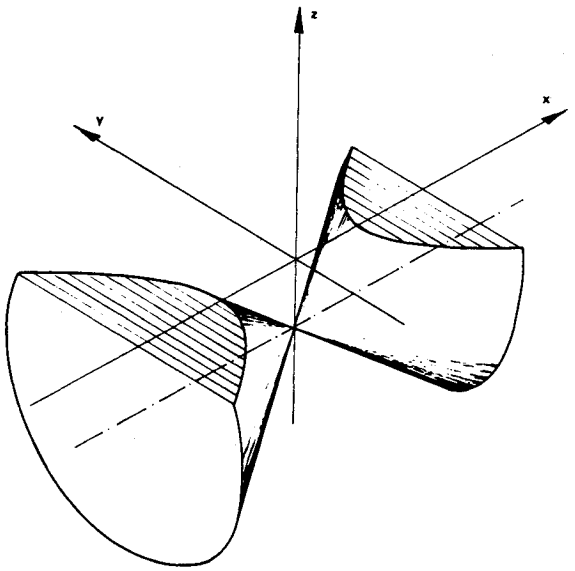

Fig. 5 Mach cones of the linear wave equation and their intersection with the plane where the initial values are given.

We can construct the solution by Fourier superposition of the modal solutions

$$\phi = \exp[i(k_1 x + k_2 y + k_3 z)]$$

in the x and y directions. But then

$$k_3 = \pm\sqrt{k_1^2 - k_2^2}$$

leads to exponential growth in the z direction when the wavenumber in the y direction, k_2, is larger than that in the x direction. In this simple model, then, we may expect the ill-posed nature of the problem to manifest itself when the y variation of the initial data is comparable to or larger than the x variation. Translating this to practical terms, we can expect the inherent instability to cause difficulty for small aspect ratio wings. Payne[10] has used energy arguments to show that exponential growth in the z direction must eventually occur for a large class of functions f and g. We demonstrate this instability in a subsequent section.

Small Disturbance Equations: An Illustration

We illustrate the procedure for computing the supersonic domain, as well as the difficulties that may arise, with the small disturbance equations. The small disturbance approximation introduces difficulties unique to this approximation; these we do not discuss. We first compute the elliptic flowfield using fictitious equations in supersonic regions to maintain elliptic behavior. While we use the Ballhaus-Bailey-Frick line relaxation algorithm as implemented by Mason et al.[8] for our computations, we use a simpler equation in this discussion, viz.,

$$-[\tfrac{1}{2}(K-\phi_x)^2]_x + [\phi_y]_y + [\phi_z]_z = 0 \tag{8}$$

When $(K-\phi_x)<0$ we make a change in the difference algorithm that corresponds to changing the first term to

$$[|\phi_x - K|^P/P]_x, \quad P \geq 1 \tag{9}$$

The sonic surface on an $AR=6$ rectangular wing corresponding to $P=2$ is shown in Fig. 6. Figure 7 shows the corresponding vertical velocity component of the redesigned airfoil for selected spanwise stations. We note that the more elliptic we make the fictitious gas (i.e., smaller P) the broader and lower the sonic surface will be. This, of course, means

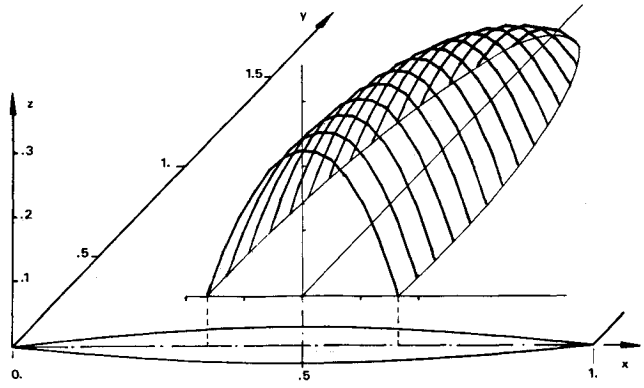

Fig. 6 Sonic surfaces for a rectangular wing with $AR=6$, $P=2$, $M_\infty=0.87$.

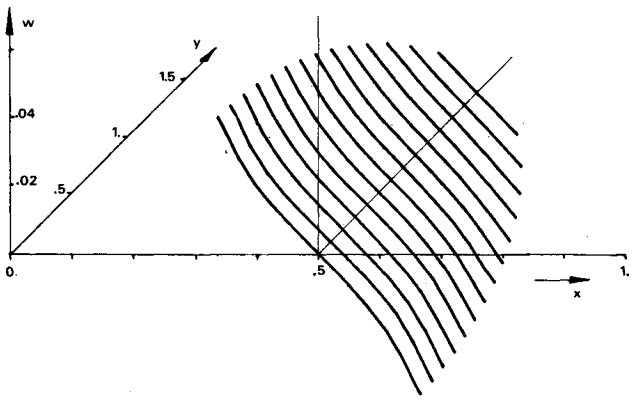

Fig. 7 New surface slopes for the rectangular wing with $AR=6$, $P=2$, $M_\infty=0.87$.

that the body will be thinner; this is reflected in the vertical velocity component. For the original parabolic arc section the body slope, and hence the vertical velocity, decrease linearly with x.

The numerical solution then provides values of ϕ, and hence its derivatives, on an embedded sonic surface, $z=z_*(x,y)$, as sketched in Fig. 6. The hyperbolic problem for the supersonic domain is solved using the simplified system of equations corresponding to Eq. (8).

$$-\tfrac{1}{2}[(K-u)^2]_x + v_y + w_z = 0, \quad w_x - u_z = 0,$$

$$w_y - v_z = 0, \quad (u_y - v_x = 0)$$

We may define a new variable $\xi(x,y)$ to replace the coordinate z, and facilitate the computations, e.g.,

$$\xi(x,y) = z/z_*(x,y)$$

In this variable the equations become

$$u_\xi = D^{-1} \begin{bmatrix} (K-u)\xi_x & 0 & 1+\xi_y^2 \\ (K-u)\xi_y & 0 & -(K-u)\xi_x\xi_y \\ -(K-u) & 0 & (K-u)\xi_x \end{bmatrix} \cdot u_x$$

$$+ \begin{bmatrix} 0 & \xi_x & -\xi_x\xi_y \\ 0 & \xi_y & 1+(K-u)\xi_x^2 \\ 0 & -1 & \xi_y \end{bmatrix} \cdot u_y \tag{10}$$

where u has the components u, v, w and $D=1+\xi_y^2+(K-u)\xi_x^2$. Our choice of the irrotationality conditions was dictated by the requirement that the determinant of the system D be nonsingular. Any other choice of equations gives $D'=\xi_y D$ and the system is singular when $\xi_y(x,y)=0$, which always occurs. Limit surfaces occur only if D changes sign. For the system considered here this occurs when $(K-u)\xi_x^2(<0)$ becomes larger in magnitude than $1+\xi_y^2$. But D may also vanish because the coordinate system used for the set of equations chosen is not the appropriate one. This failure can be remedied by another choice for the coordinate system and must not be confused with that which occurs when a true limit line is present.

As discussed earlier, the initial value problem we solve is ill-posed. The implied numerical instability becomes more serious when the spanwise gradients are large. Indeed, as we can see from Eq. (10),

$$u_\xi = D^{-1}\{(K-u)\xi_x u_x + (1+\xi_y^2)w_x + \xi_x v_y - \xi_x\xi_y w_y\} \quad (11)$$

$$- \quad \pm\pm \quad + \quad - \quad \pm\pm \quad \pm - \mp$$

Consider the sign of the individual terms on the right-hand side for an unswept rectangular wing with a profile symmetrical about the midchord and midspan lines. (The upper/lower sign corresponds to ahead of/behind the midchord line.) Then, because we are solving an elliptic boundary-value problem where the terms have the indicated signs, all of the terms in Eq. (11) except $\xi_x v_y$ give $u_\xi<0$. The smaller the aspect ratio the larger the local values of $\xi_x v_y$. A similar conclusion holds for v, with a $\xi_y v_y$ term providing a change in v_ξ that increases v and v_y. With a spanwise instability present in the numerics we can anticipate that as it grows in amplitude v_y will grow and affect the magnitude, and eventually the sign, of u_ξ. Figure 8 depicts the surface values $u(x,y,0)$ computed for the supersonic region on rectangular wings of aspect ratios 3 and 2. For an aspect ratio 2 wing numerical instabilities obviously override the generally smooth nature of the flow. Inspection of the other velocity components strongly suggests that the instability has a wavelength four times that of the spanwise grid spacing and amplifies v more rapidly than u or w. The initial data for the two cases are similar, except for the larger y gradients when $\mathcal{R}=2$.

Wing Design

The art of aircraft wing design involves many variables and requires knowledge and expertise beyond that of the authors. We believe, however, that by using fictitious equations with suitable baseline configurations various design goals can be met and the wings will be shock free at reasonable flight Mach numbers and lift coefficients. To aid the aircraft designer in understanding this technology we briefly describe the shock-free design process for a simple wing.

The approach outlined in the previous sections results in wings and airfoils with upper surface curvatures that are less than those of the baseline configurations. Additionally, the more acute the intersection of the sonic surface with the body surface, the less the likelihood of a limit surface intervening between the sonic line and the body. For this reason, baseline configurations should have reasonable upper surface curvatures and more thickness than required by the final designs. Designs that are close to the limit of what can be achieved, in terms of Mach number and lift coefficient, will have limit surfaces that nearly penetrate the wing surface. This may occur near the leading edge of the wing or near the aft end of the supersonic region, or in both locations simultaneously.

We will illustrate some of these points with a simple tutorial example. We take a well known airfoil, the 64A4xx, and use it for the wing sections. The planform is chosen to have straight

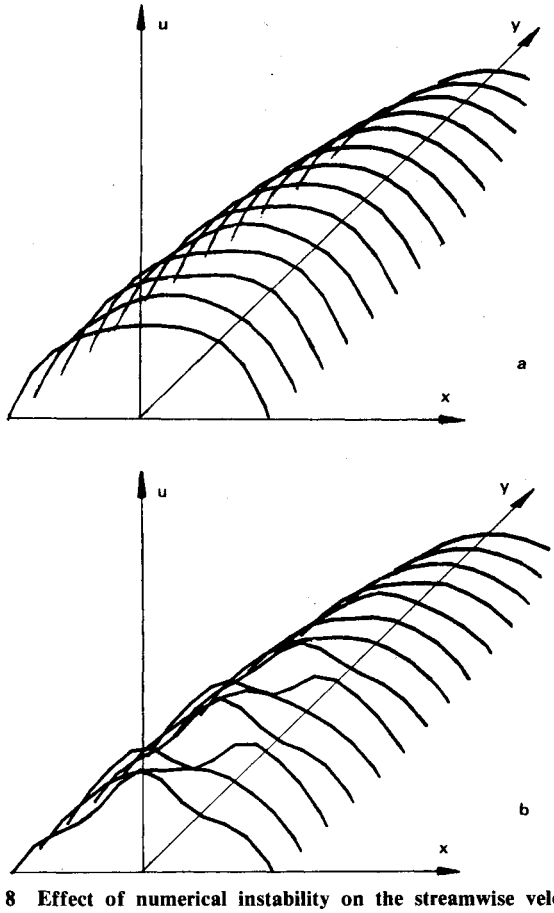

Fig. 8 Effect of numerical instability on the streamwise velocity component for: a) $\mathcal{R}=3$, $M_\infty=0.88$; b) $\mathcal{R}=2$, $M_\infty=0.89$. There is no evidence of instability when $\mathcal{R}=6$, $M_\infty=0.87$.

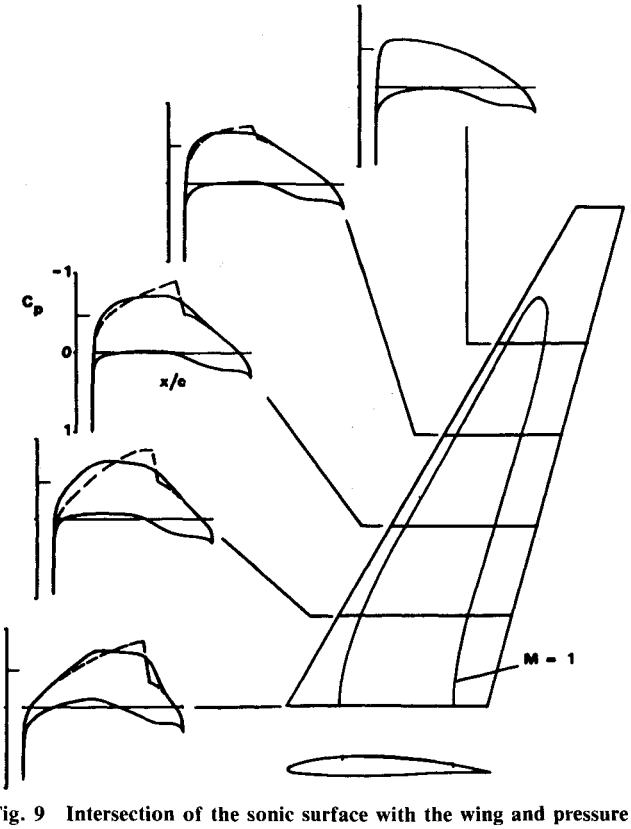

Fig. 9 Intersection of the sonic surface with the wing and pressure coefficients for: the wing designed to be shock free ——; the baseline wing ———; $M_\infty=0.80$.

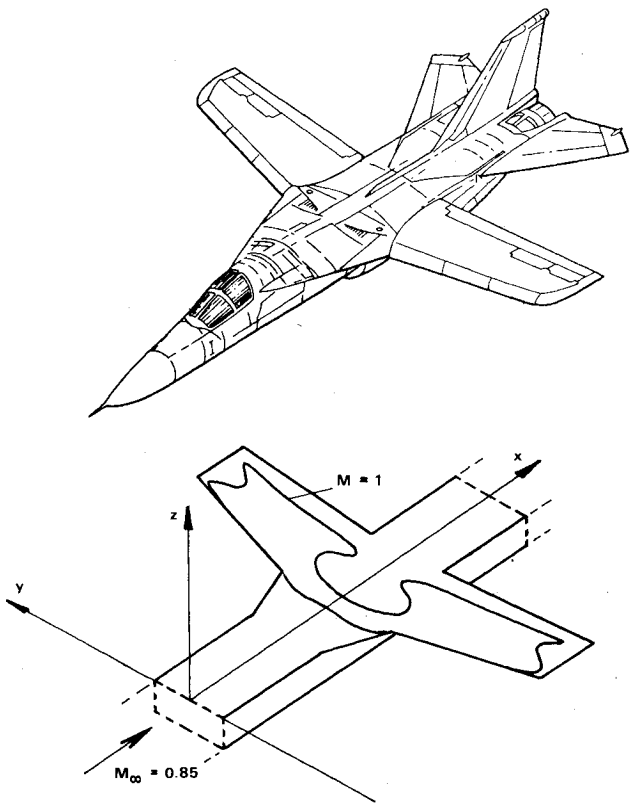

Fig. 10 Sonic surface on the supercritical wing of the AFTI 111 using fictitious equation in the supersonic region.

leading and trailing edges with sweep angles of 30 and 15 deg, respectively. We take the aspect ratio based on wing area to be 8, and the thickness distribution to be elliptical and 10% thick at the wing root. The twist is varied from 4 deg at the root section to 0 deg at midspan, and the angle of attack is 0.4 deg. With a freestream Mach number of 0.80 these conditions will lead [at least for the fictitious equations with $P=2$ in Eq. (9)] to sonic surface data for the system Eq. (10) that are consistent with shock-free flow; that is, no limit surface intervenes before the wing surface is found. Figure 9 shows the intersection of the sonic surface found with the wing, and the center sections of both the baseline configuration and the shock-free design. The design wing is 0.7% of the chord thinner than the baseline wing at the center section. Also shown is a comparison of the pressure coefficient at selected span stations. Both wings have a lift coefficient of 0.50. The small modifications to the baseline wing, over the portion of the upper surface wetted by supersonic flow in the solution of the fictitious equations, results in a wing, that when analyzed numerically, has the shock-free pressure distribution shown. The pressure coefficient on the baseline configuration is also shown for comparison. The inviscid drag evaluation for the original wing gave 96 counts; that for the design wing 86 counts, reflecting the changes in the pressure coefficient. Presumably a viscous calculation that correctly modeled the shock-wave boundary-layer interaction would reflect further improvements.

The selection of a baseline configuration is important to the success of this method. Wings that employ traditional supercritical airfoils will lead to sonic surface data that result in a limit surface. Figure 10 shows the intersection of the sonic surface with the wing for the AFTI 111 wing; again we have used the fictitious equations with $P=2$. The complex nature of this surface, and the occurrence of a limit surface when redesign is attempted, is due to the supercritical design of the AFTI 111 wing. Modifications to the baseline configuration, such as this one, are essential ingredients of any attempt at shock-free design. This is illustrated further in Ref. 9, where analytical functions are used to modify supercritical airfoils.

Conclusion

A procedure for designing wings that are shock free has been described in general terms and illustrated by using the small perturbation equations to modify a simple baseline configuration so that it is shock free. In using this procedure the designer must select the baseline configuration to be modified and the fictitious equations to be used. These determine the flowfield on the sonic surface of the ultimate design. A good choice will allow high Mach numbers and lift coefficients to be obtained. A poor choice will result in a limit surface in the supersonic domain at the design Mach number and lift coefficient. Instabilities in the numerical calculation of the supersonic flow that provides the wing design occur whenever the spanwise gradients are large. These can be suppressed by smoothing both the chordwise and spanwise data at each successive step of the calculation.

Acknowledgments

This research was carried out by the Computational Mechanics Laboratory of the Department of Aerospace and Mechanical Engineering under AFOSR Grant 76-2954G and ONR Grant N00014-76-C-0182.

References

[1] Sobieczky, H., Fung, K-Y., Yu, N. J., and Seebass, A. R., "A New Method for Designing Shock-Free Transonic Configuration," *AIAA Journal*, Vol. 17, July 1979, pp. 722-729.

[2] Yu, N. J., "An Efficient Transonic Shock-Free Wing Redesign Procedure Using a Fictitious Gas Method," *AIAA Journal*, Vol. 18, Feb. 1980, pp. 143-148.

[3] Yu, N. J. and Rubbert, P. E., "Transonic Wing Redesign Using a Generalized Fictitious Gas Method," Boeing Document D-180-25309-1, May 1979.

[4] Sobieczky, H., "Die Berechnung lokaler räumlicher Überschallfelder," ZAMM 58T, 1978.

[5] Sobieczky, H., "A Computational Algorithm for Embedded Supersonic Domains," University of Arizona Engineering Experiment Station Rept. TFD 78-03, 1978.

[6] Jameson, A. and Caughey, D. A., "Numerical Calculations of the Transonic Flow Past a Swept Wing," NASA CR-153297, 1977.

[7] Caughey, D. A. and Jameson, A., "Numerical Calculation of Transonic Potential Flow About Wing-Body Combinations," *AIAA Journal*, Vol. 17, Feb. 1979, pp. 175-181.

[8] Mason, W. H., Mackenzie, D., Stern, M., Ballhaus, W. F., and Frick, J., "An Automated Procedure for Computing the Three-Dimensional Transonic Flow Over Wing-Body Combinations, Including Viscous Effects," Vols. I and II, Air Force Flight Dynamics Laboratory, Wright-Patterson Air Force Base, AFFDL-TR-77, Ohio, 1978.

[9] Sobieczky, H., "Related Analytical Analog and Numerical Methods in Transonic Airfoil Design," AIAA Paper 79-1556, July 1979.

[10] Payne, L. E., private communication, Cornell University, Sept. 1978.